CONFIDENTIAL

Copy 6
RM E55E05

NACA RM E55E05

UNCLASSIFIED

NACA

RESEARCH MEMORANDUM

EFFECT OF INLET TEMPERATURE ON ROTATING STALL AND BLADE VIBRATIONS IN A MULTISTAGE AXIAL-FLOW COMPRESSOR

By Arthur A. Medeiros, Howard F. Calvert, and David B. Fenn

Lewis Flight Propulsion Laboratory
Cleveland, Ohio

CLASSIFICATION CHANGED
UNCLASSIFIED

To ____________________

By authority of TPA #39 Date 1/12/61

CLASSIFIED DOCUMENT

NATIONAL ADVISORY COMMITTEE FOR AERONAUTICS

WASHINGTON
August 5, 1955

CONFIDENTIAL

UNCLASSIFIED

NATIONAL ADVISORY COMMITTEE FOR AERONAUTICS

RESEARCH MEMORANDUM

EFFECT OF INLET TEMPERATURE ON ROTATING STALL AND BLADE VIBRATIONS IN A MULTISTAGE AXIAL-FLOW COMPRESSOR

By Arthur A. Medeiros, Howard F. Calvert, and David B. Fenn

SUMMARY

Rotating-stall and blade-vibration data for the first three rotor blade rows of a 13-stage axial-flow compressor were obtained at inlet temperatures of -50°, 60°, and 155° F. The stall frequency for a given stall pattern was found to be essentially a linear function of actual engine speed and was independent of inlet temperature. However, the actual speed range over which a given stall pattern was obtained shifted with the various inlet temperatures investigated. The speed range for a given stall pattern could be uniquely defined by equivalent engine speed. The ratio of stall speed to engine speed was approximately constant for a given stall configuration and varied from 0.47 to 0.55 for stall patterns consisting of one to five zones.

The speeds at which resonant blade vibrations in the first three stages of rotor blades could occur were determined from critical-speed diagrams and verified by strain-gage measurements. The critical speeds were independent of inlet temperature. However, because the stall pattern at a given speed is a function of inlet temperature, resonant vibrations at the critical speed would occur only over the temperature range where the stall zone responsible for the resonant condition was encountered.

INTRODUCTION

The investigations reported in references 1 to 3 show that stall of a blade row results in low-flow regions (stall zones) that are usually symmetrically spaced around the circumference of the blade row. The low-flow zones propagate around the blade row from the pressure surface to the suction surface of the blades. Because of the relative motion between the symmetrically spaced stall zones and the blades, each blade experiences a periodic fluctuation of loading. References 4 to 7 show the correlation of the periodic loading of rotating stall with resonant blade vibrations. In some instances these vibrations have resulted in fatigue failures.

In multistage compressors the stall-propagation velocity has been found to be in the relatively narrow range from 45 to 57 percent of the rotor speed. The number of zones in the stall pattern, however, has varied from 1 to 8 (refs. 6 to 8), so that a large range of blade excitation frequencies is possible.

The natural frequency of the rotor blades of a compressor is a function of the actual rotational speed of the rotor blade row. The natural frequency increases with speed because of the stiffening effect of centrifugal force. The aerodynamic operating condition of the compressor, however, is a function of equivalent speed. The equivalent speed is defined as the actual speed divided by the square root of the ratio of inlet temperature to standard sea-level temperature (59° F). Thus, inlet temperature may have a definite effect on stall-incited blade vibrations because of the many combinations of actual and equivalent speeds that are possible. For this reason, it is desirable to determine a correlation of inlet temperature and stall characteristics and attendant blade vibrations. 3605

The investigation reported herein, conducted at the NACA Lewis laboratory, is concerned with the effects of inlet temperature on stall frequency and blade vibration. A 13-stage axial-flow compressor was run as part of a turbojet engine at inlet temperatures of -50°, 60° and 155° F. The Reynolds number index for the two extreme temperatures was 0.46 and for the intermediate temperature, 0.89. The Reynolds number index is defined as $\frac{P/P_{sl}}{(T/T_{sl})(\mu/\mu_{sl})}$, where P, T, and μ are inlet pressure, temperature, and viscosity, respectively. The subscript sl indicates sea-level standard conditions. The investigation covered a speed range from approximately 55 to 75 percent of rated equivalent design speed. The highest equivalent speed is the maximum at which rotating stall was encountered along the equilibrium engine operating line with rated nozzle area. Data were obtained to determine the number of stall zones present in the compressor, the stall frequency, and the vibratory stresses in the first three rotor rows.

APPARATUS AND PROCEDURE

Installation

The axial-flow compressor used for the investigation reported herein consisted of 13 stages and was run as part of a turbojet engine in an altitude test chamber. The engine was fitted with an adjustable-area exhaust nozzle, so that the compressor operating point at any given speed could be varied.

Instrumentation

The flow fluctuations of rotating stall were measured by the use of a constant-current hot-wire anemometer. The anemometer signals were recorded on a 24-channel recording oscillograph. Each anemometer probe was fitted with a 0.001-inch-diameter by 0.10-inch-long wire. The wire was kept at a constant average temperature. The flow fluctuations were detected from the instantaneous variations in wire temperature (resistance). A resistance-capacitor compensator was used to obtain the necessary speed of response.

Anemometer probes were located in the stator passage of the first, second, and third stages. Three angular spacings of the probes were provided in each stage. The number of stall zones was determined by the method shown in reference 2.

The blade stresses were measured in the first three rotor stages by the use of resistance-wire strain gages. The strain gages were installed on 24 rotor blades equally divided among the three stages in two diametrically opposite groups of four blades each. Lead wires from the gages were run to a slip-ring assembly mounted on the front of compressor. The slip-ring assembly and strain-gage circuit are described in reference 9.

Procedure

The engine was run over a range of speeds from approximately 55 to 75 percent of rated equivalent speed. The exhaust-nozzle area was varied at each speed from that required for rated operation to that for limiting exhaust-gas temperature at approximately 75 percent of equivalent design speed. The inlet conditions are as follows:

Temperature, $^{\circ}F$	Reynolds number index
155	0.46
60	.89
-50	.46

RESULTS AND DISCUSSION

Rotating-Stall Characteristics

The absolute stall frequencies measured in this investigation are plotted in figure 1 as a function of engine speed. The data for the standard temperature (60° F) were reported in reference 6. Stall configurations consisting of 1, 2, 3, 4, and 5 stall zones were detected. The various stall configurations were obtained by varying both speed and exhaust-nozzle area, so that more than one stall pattern could be obtained at a given engine speed. The absolute stall frequency for any given stall configuration (number of stall zones) increases linearly, within experimental scatter, with compressor speed. The different inlet conditions had no apparent effect on the linear relation between flow-fluctuation frequency and compressor speed. The greatest effect of inlet conditions is the change in the compressor speed range at which stall is encountered. As the inlet temperature is increased, the maximum speed at which stall occurs also increases. 3605

The increased engine speed at which stall is encountered can be anticipated on the basis of compressor theory. For a given ram pressure ratio, the operating point of the compressor (pressure ratio and equivalent weight flow) in a turbojet engine is uniquely defined by equivalent speed and exhaust-nozzle area, disregarding effects of Reynolds number. Equivalent flow and equivalent speed determine the stall configuration encountered in a particular compressor. With a given exhaust-nozzle area, therefore, the same stall configuration can be expected at a given equivalent speed. Thus, the absolute, or actual, engine speed range over which a stall configuration is encountered is a function of inlet temperature. The higher the inlet temperature, the higher the actual speed at which rotating stall will be encountered with a given exhaust-nozzle area. Since the stall frequency can be considered an aerodynamic velocity, it can further be expected that, at a given equivalent engine speed and exhaust-nozzle area, the same equivalent stall frequency $(f_s/\sqrt{\theta})$ would be obtained.

The equivalent stall frequencies measured with the three inlet temperatures are plotted in figure 2 against equivalent compressor speed. At any given equivalent compressor speed, the same equivalent stall frequency is obtained for a given stall configuration, regardless of the inlet temperature. The speed limits over which a given stall characteristic is obtained are slightly different, because testing limitations did not permit a choice of exhaust-nozzle area that is independent of inlet conditions. The minimum area was fixed by limiting exhaust-gas temperature, and the maximum area was limited by the necessary ram pressure ratio required across the test installation. In general, however, the range of equivalent speeds over which a given stall pattern exists is independent of inlet temperature.

The ratio of stall velocity $h = f_s/\lambda$ to compressor speed is plotted against equivalent compressor speed in figure 3 (λ is the number of stall zones in the pattern). With the exception of a few scattered points, the stall-velocity to compressor-speed ratio is constant over the equivalent-speed range for any given stall configuration. The average speed ratio for each of the five stall configurations is as follows:

Stall zones, λ	Ratio of stall velocity to rotor speed, h/N
1	0.470
2	.525
3	.525
4	.54
5	.55

3605 The range of speed ratios is relatively narrow and falls within the range previously encountered in multistage compressors.

Data obtained on multistage compressors presented in the form of figures 2 and 3 would represent a satisfactory calibration of rotating-stall frequencies obtainable in that particular compressor, regardless of the inlet temperature at which the data were obtained. It would be necessary, of course, to determine the exact equivalent-speed limits to which each of the stall configurations is confined for a given exhaust-nozzle area.

Blade Vibration

The effect of inlet temperature on rotating stall may be interpreted with respect to its effect on resonant blade vibration. The engine speeds at which resonant vibrations could occur in a particular blade row can be determined from a plot of the ratio of rotating-stall frequency to natural bending frequency of the blades against engine speed. In the case of a rotor blade row the relative stall frequency must be used:

$$f_s' = N\lambda - f$$

where f_s' is the stall frequency relative to rotor blades, f is the absolute stall frequency, N is the engine speed, and λ is the number of stall zones in the stall pattern. In addition, the natural bending frequency of the blades should be corrected for the stiffening effect of centrifugal force (see ref. 10).

Critical-speed diagrams for the first three rotor blade rows for the compressor used in this investigation are shown in figure 4. The relative stall frequencies were calculated from the absolute stall frequencies obtained from figure 1 and extrapolated linearly for an engine speed range from 3000 to 8300 rpm. Inasmuch as the wave form of the force variation resulting from rotating stall contains strong harmonics and is not simply sinusoidal, the blades can be excited to resonant vibration not only when the stall and natural bending frequencies are equal but also when the stall frequency is some fraction (e.g., 1/2, 1/3, etc.) of the natural frequency of the blades. The number of harmonics that must be considered depends on the particular shape and strength of the wave form due to rotating stall.

The critical speeds obtained from figure 4 are listed in the following table. Resonance with the fundamental and first harmonic only are considered:

Stage	Engine speed, rpm	Stall zones	Type of resonance
1	7550	5	Fundamental
	3730	4	First harmonic
	5190	3	First harmonic
2	3250	5	First harmonic
	4150	4	First harmonic
	5800	3	First harmonic
3	4150	5	First harmonic
	5270	4	First harmonic
	7550	3	First harmonic

Although these critical speeds are all possible, the inlet temperature must be such that, at the given critical speed, the equivalent speed is in the range where the stall zone responsible for resonant vibration is present. This necessary condition is illustrated in figure 5 for the case of the three-zone stall pattern. Engine speed is plotted against inlet total temperature. An auxiliary scale presents the flight Mach number that would give the corresponding inlet total temperature for flight in the tropopause. Two lines of constant equivalent speed (4780 and 6140 rpm) are shown; these are the equivalent-speed limits over which three stall zones can be obtained as indicated in figure 2. In addition, three lines of constant actual speed (5190, 5800, and 7550 rpm) are shown, which correspond to the critical speeds for the first, second, and third stages, respectively.

Figure 5 indicates that resonant blade vibration in the first stage, due to three stall zones, can be expected over an inlet-temperature range from approximately -90° to 160° F. The effective inlet-temperature range for three-stall-zone excitation in the second stage is from approximately 5° to 310° F. In the third stage resonant excitation with the first harmonic of the three stall zones could be expected only at some inlet temperature above 340° F, which corresponds to a flight Mach number in the tropopause of approximately 2.3. Diagrams similar to figure 5 could be made for each stall configuration to determine the temperature ranges over which blade vibrations due to rotating stall could be encountered.

The maximum vibratory stresses measured in each of the first three stages are shown in figure 6. In the first stage, the maximum stress occurs at 5200 rpm and is due to resonance with the first harmonic with three stall zones; this agrees with the critical speed shown in figure 4(a). The level of maximum vibratory stress varies because of the different inlet-air densities for the three sets of data. Peak stresses are encountered at 5200 rpm over the entire range of inlet temperature run. From figure 5 it would be expected that an inlet temperature just slightly above the maximum run (155° F) would be sufficient to put the critical speed outside the equivalent-speed range for three stall zones; therefore, high vibratory stresses would not be encountered in the first stage.

In the second stage, the maximum vibratory stress occurs at 5800
3605 rpm. Figure 4(b) indicates that the high stress at this speed is due to resonance with the first harmonic of three stall zones. The inlet-temperature range over which 5800 rpm is critical is from 5° to 310° F (fig. 5); consequently, at the lowest inlet temperature used in this investigation (-50° F), high vibratory stresses are not encountered.

In the third stage, high stresses are encountered at 5200 rpm only with the intermediate temperature. Figure 4(c) shows that the resonant condition on the third stage at this speed occurs because of the first harmonic of four stall zones. The equivalent-speed range for four stall zones is 4570 to 5850 rpm. The temperature range, then, over which high vibratory stresses might be encountered at 5200 rpm is from -50° to 210° F. The lower temperature used in the investigation was sufficiently close to the low-temperature limit to explain why high stresses were not encountered with the cold inlet temperature (-50° F). However, the runs made at high inlet temperature (155° F) were within the range where high stresses would have been measured at the critical speed. With the high inlet temperature, the minimum exhaust-nozzle area run was limited by high exhaust-gas temperatures; consequently, the compressor did not operate in the region where four stall zones would be prevalent.

The stall and blade-vibration data reported herein indicate that the stall frequency is a function only of the stall pattern and the absolute compressor speed. The absolute speed at which resonant blade vibrations excited by a particular stall pattern can be encountered does not change with inlet temperature; however, the speed at which the particular stall pattern can be obtained depends on inlet temperature.

SUMMARY OF RESULTS

An investigation to determine the effects of inlet temperature on rotating stall and associated blade-vibration characteristics of a multistage axial-flow compressor produced the following results:

1. Stall patterns consisting of 1, 2, 3, 4, and 5 stall zones were detected at all inlet temperatures in the equivalent compressor speed range between 4600 and 6200 rpm. The actual speed range over which a given stall pattern was encountered was determined by equivalent engine speed and inlet temperature.

2. The stall frequency for a given stall configuration was essentially proportional to actual engine speed and was independent of the compressor-inlet temperature. The ratio of stall speed to engine speed was essentially constant for a given stall pattern and varied from 0.47 for the one-zone pattern to 0.55 for the five-zone stall pattern.

3. Critical-speed diagrams and vibratory-stress measurements showed that resonant blade vibrations could occur in the first-stage rotor blades at 5200 rpm and in the second-stage rotor blades at 5800 rpm. In both cases, resonance was a result of the first harmonic of the three-zone stall pattern. The critical speed for the third-stage rotor blades was 5200 rpm and was a result of the first harmonic of the four-zone stall pattern.

3605

4. The critical speed at which the blade vibrations due to a given rotating-stall pattern can occur is independent of inlet temperature. The existence of the given stall pattern at that speed, however, depends on the compressor-inlet temperature.

Lewis Flight Propulsion Laboratory
National Advisory Committee for Aeronautics
Cleveland, Ohio, May 9, 1955

REFERENCES

1. Grant, Howard P.: Hot Wire Measurements of Stall Propagation and Pulsating Flow in an Axial Flow Inducer-Centrifugal Impeller System. Pratt and Whitney Res. Rep. No. 133, June 1951.

2. Huppert, Merle C.: Preliminary Investigation of Flow Fluctuation During Surge and Blade Row Stall in Axial-Flow Compressors. NACA RM E52E28, 1952.

3. Huppert, Merle C., and Benser, William A.: Some Stall and Surge Phenomena in Axial-Flow Compressors. Jour. Aero. Sci., vol. 20, no. 12, Dec. 1953, pp. 835-845.

4. Johnson, Donald F., and Costilow, Eleanor L.: Experimental Determination of Aerodynamic Forces Normal to the Chord Due to Rotating Stall Acting on Compressor Blading. NACA RM E54F14, 1954.

5. Huppert, Merle C., Johnson, Donald F., and Costilow, Eleanor L.: Preliminary Investigation of Compressor Blade Vibration Excited by Rotating Stall. NACA RM E52J15, 1952.

6. Calvert, Howard F., Braithwaite, Willis M., and Medeiros, Arthur A.: Rotating-Stall and Rotor-Blade-Vibration Survey of a 13-Stage Axial-Flow Compressor in a Turbojet Engine. NACA RM E54J18, 1955.

7. Huntley, S. C., Huppert, Merle C., and Calvert, Howard F.: Effect of Inlet-Air Baffles on Rotating-Stall and Stress Characteristics of an Axial-Flow Compressor in a Turbojet Engine. NACA RM E54G09, 1955.

8. Huppert, Merle C., Costilow, Eleanor L., and Budinger, Ray E.: Investigation of a 10-Stage Subsonic Axial-Flow Research Compressor. III - Investigation of Rotating Stall, Blade Vibration, and Surge at Low and Intermediate Compressor Speeds. NACA RM E53C19, 1953.

9. Meyer, André J., Jr., and Calvert, Howard F.: Vibration Survey of Blades in 10-Stage Axial-Flow Compressor. II - Dynamic Investigation. NACA RM E8J22a, 1949. (Supersedes NACA RM E7D09.)

10. Timoshenko, Stephen: Vibration Problems in Engineering. Second ed., D. Van Nostrand Co., Inc., 1937, p. 386.

3605

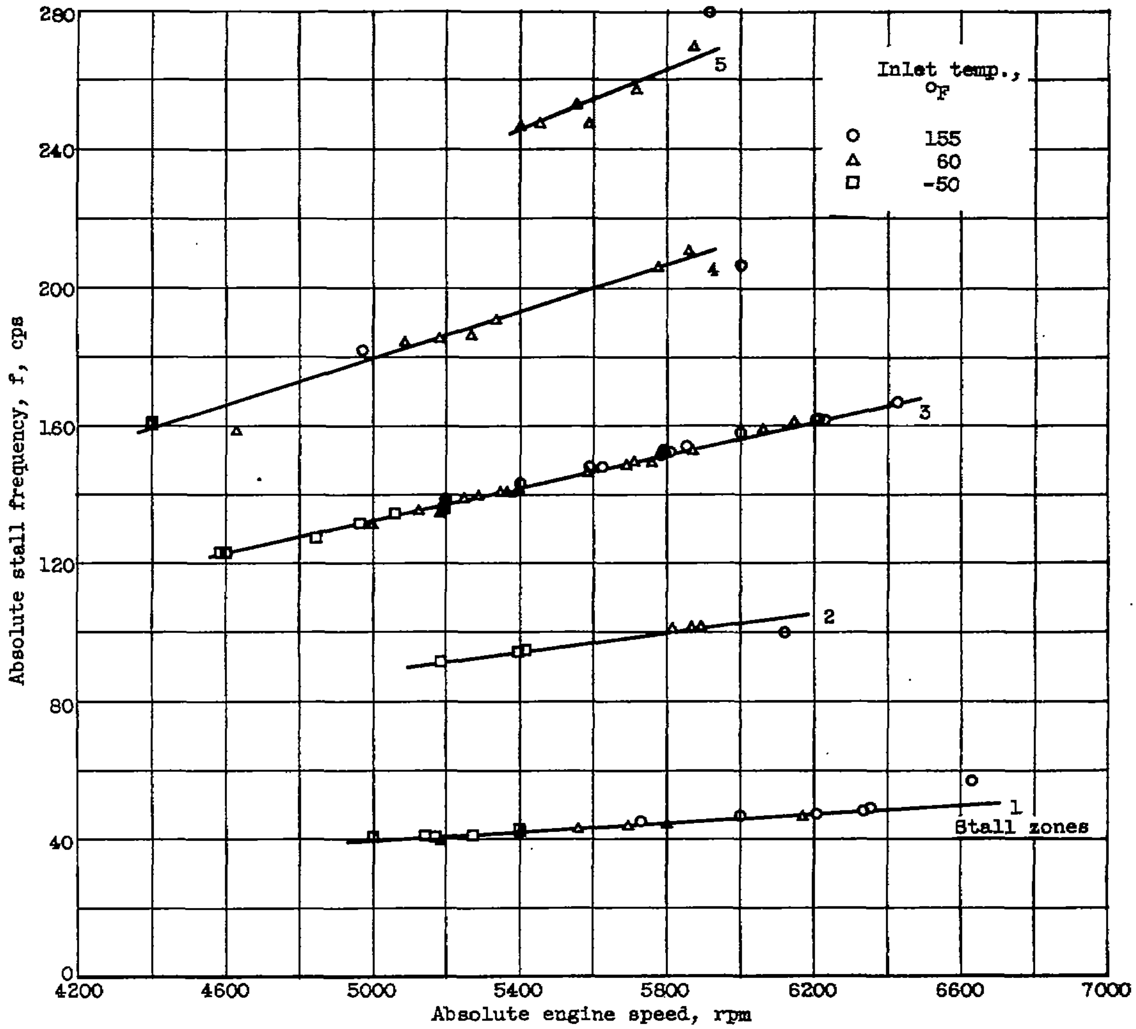

Figure 1. - Variation of stall frequency with engine speed and stall configuration.

3605

CG-2 back

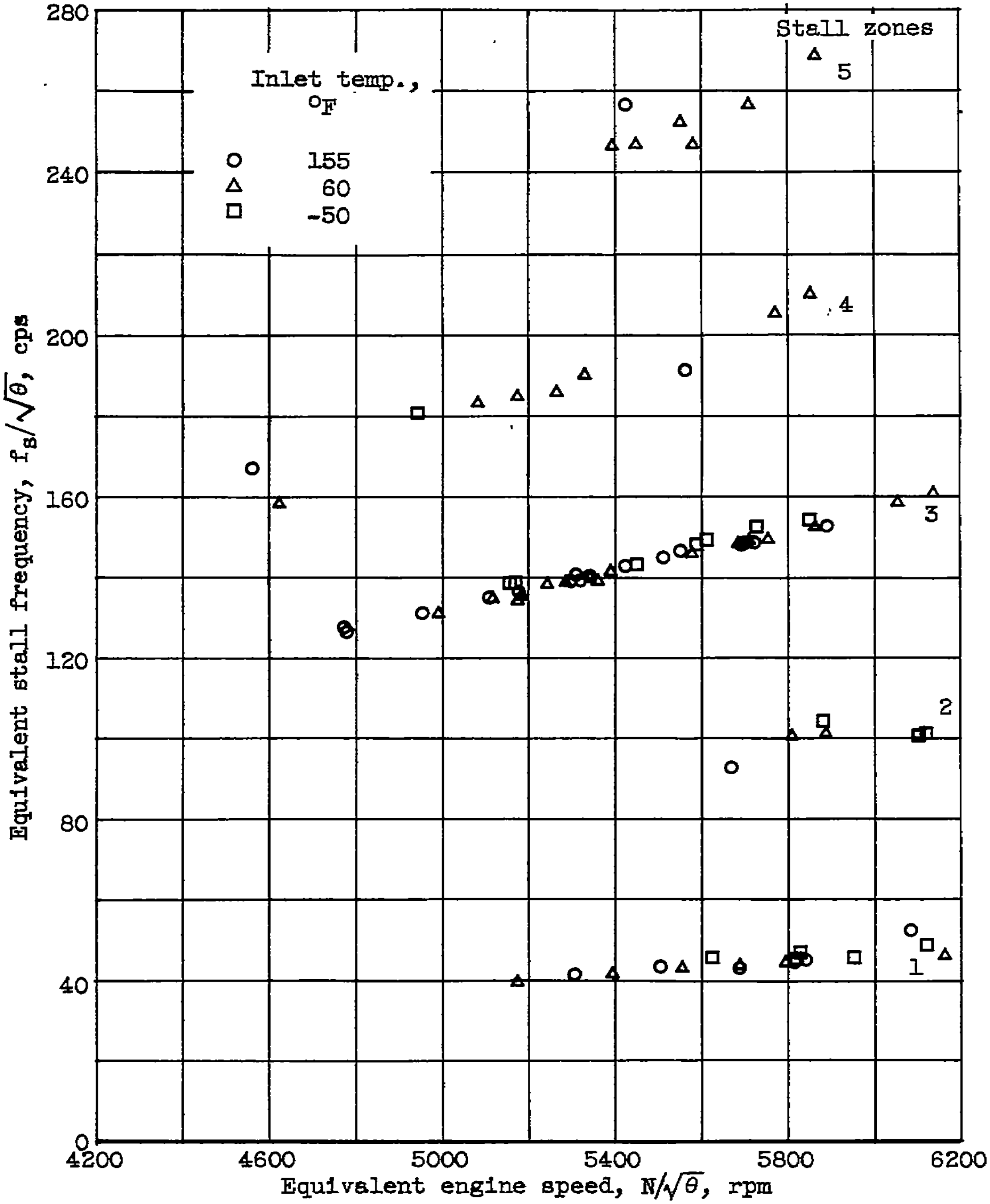

Figure 2. - Correlation of equivalent stall frequency with equivalent engine speed.

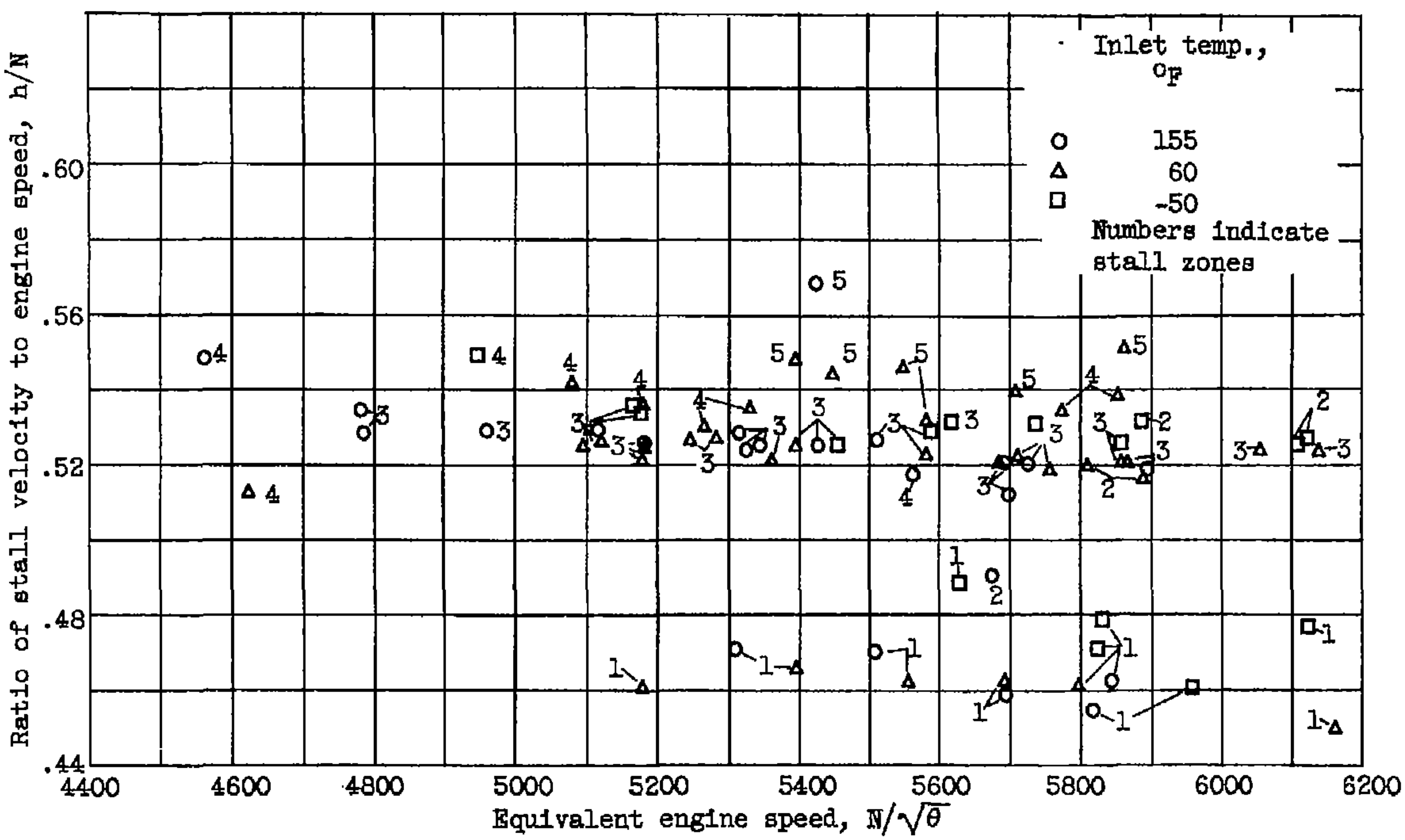

Figure 3. - Variation of ratio of stall velocity to engine speed with equivalent engine speed.

[redacted]

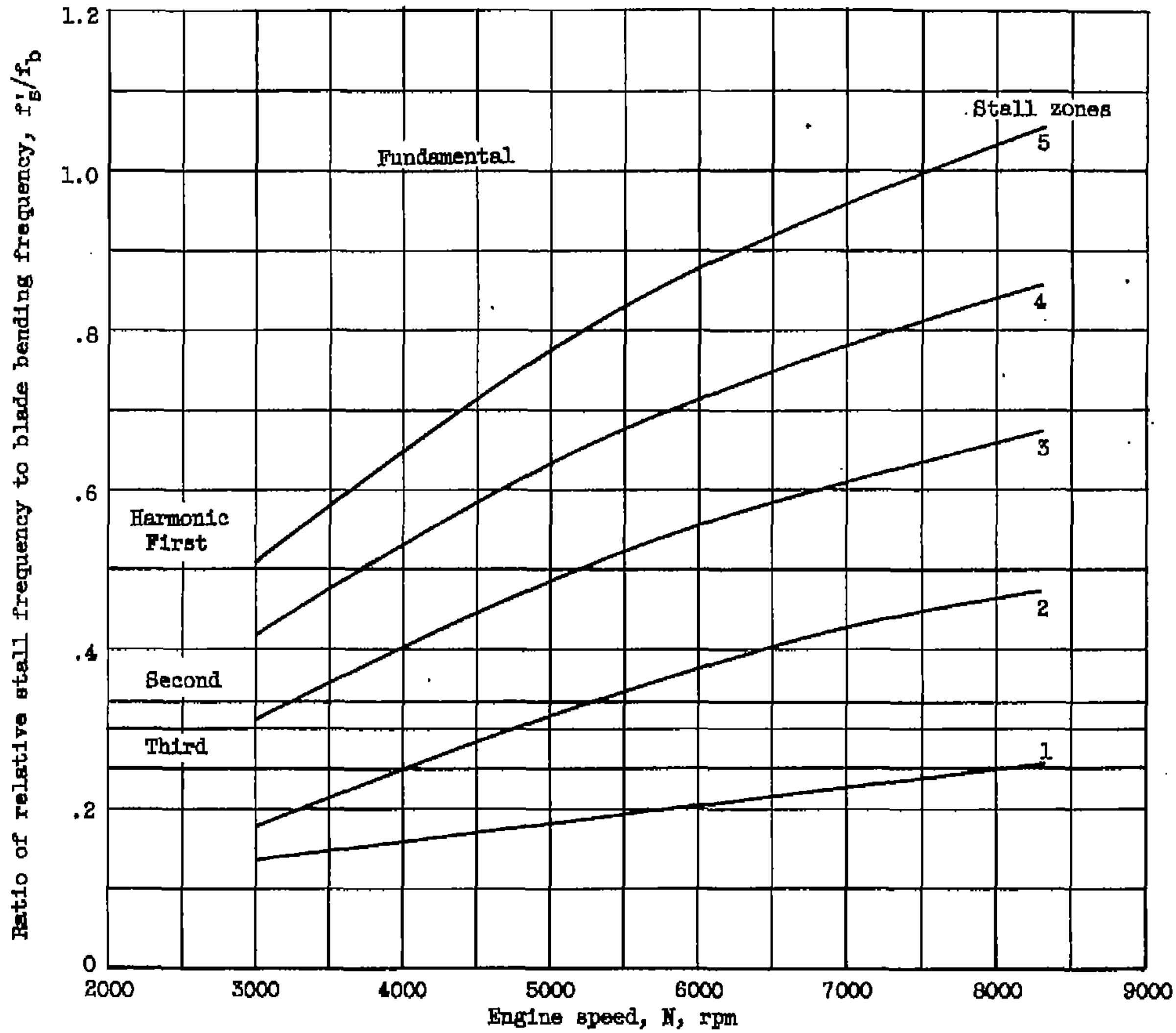

(a) First-stage rotor.

Figure 4. - Critical-speed diagrams.

[redacted]

[redacted]

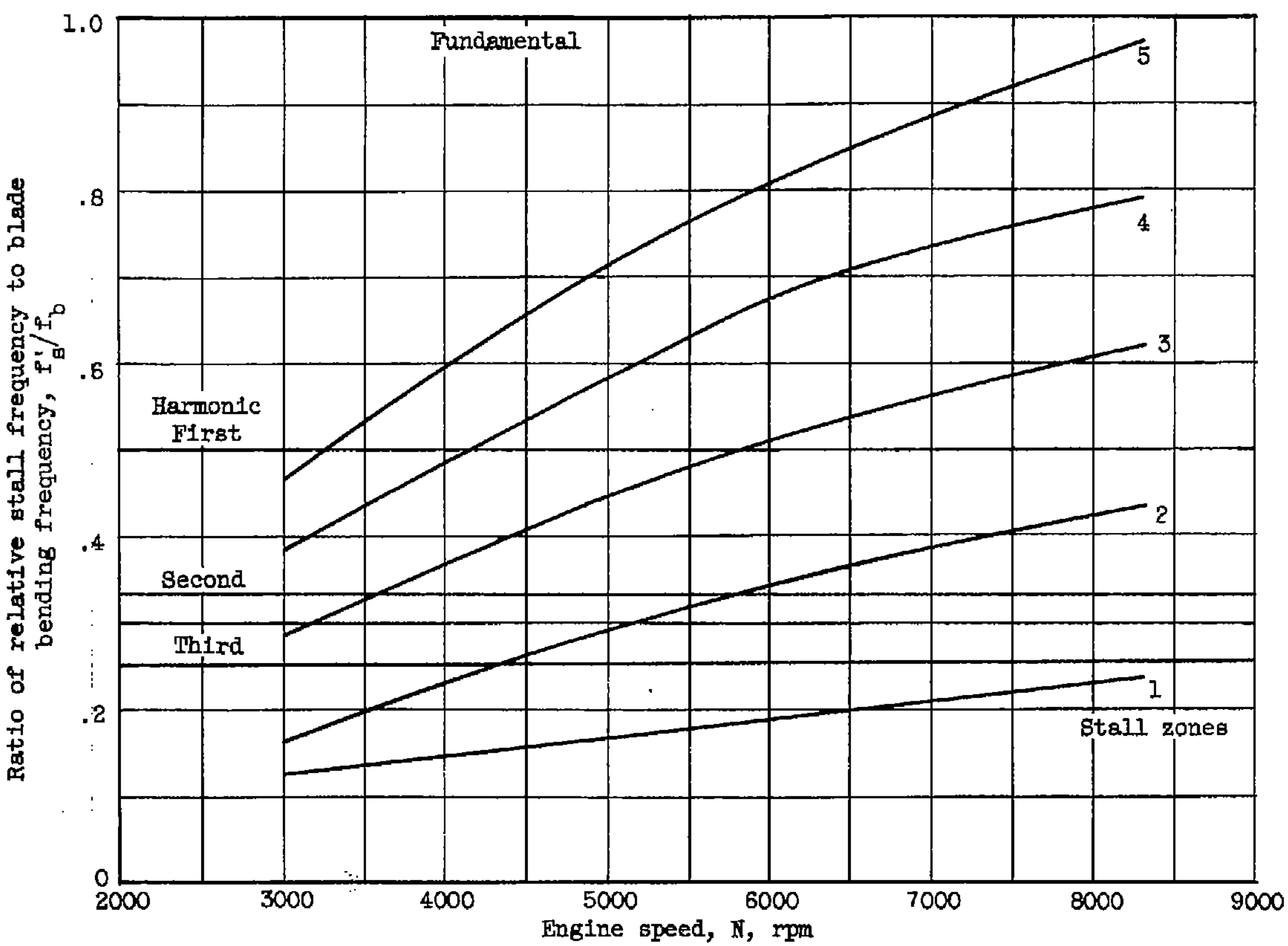

(b) Second-stage rotor.

Figure 4. - Continued. Critical-speed diagrams.

[redacted]

[redacted]

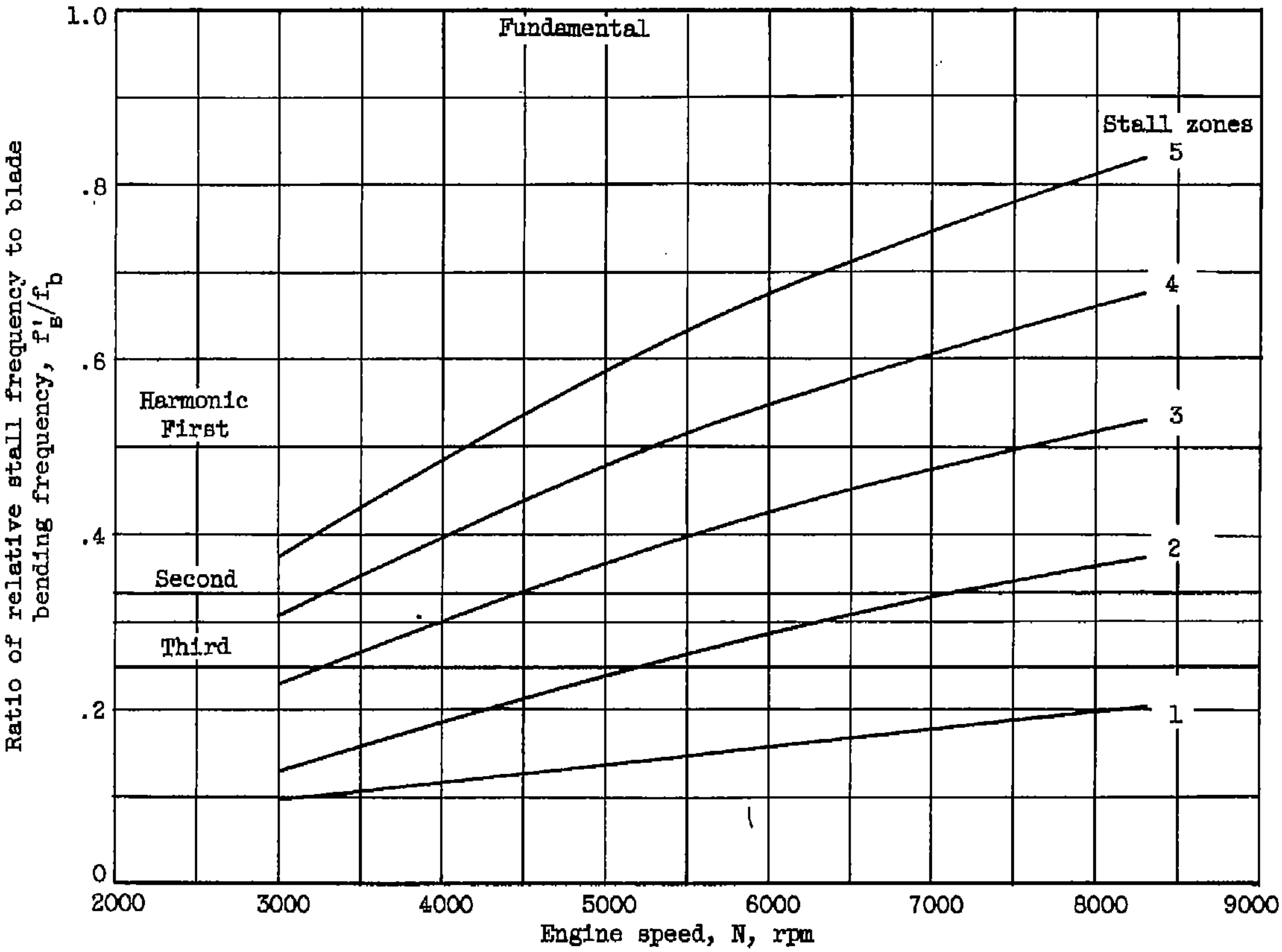

(c) Third-stage rotor.

Figure 4. - Concluded. Critical-speed diagrams.

[redacted]

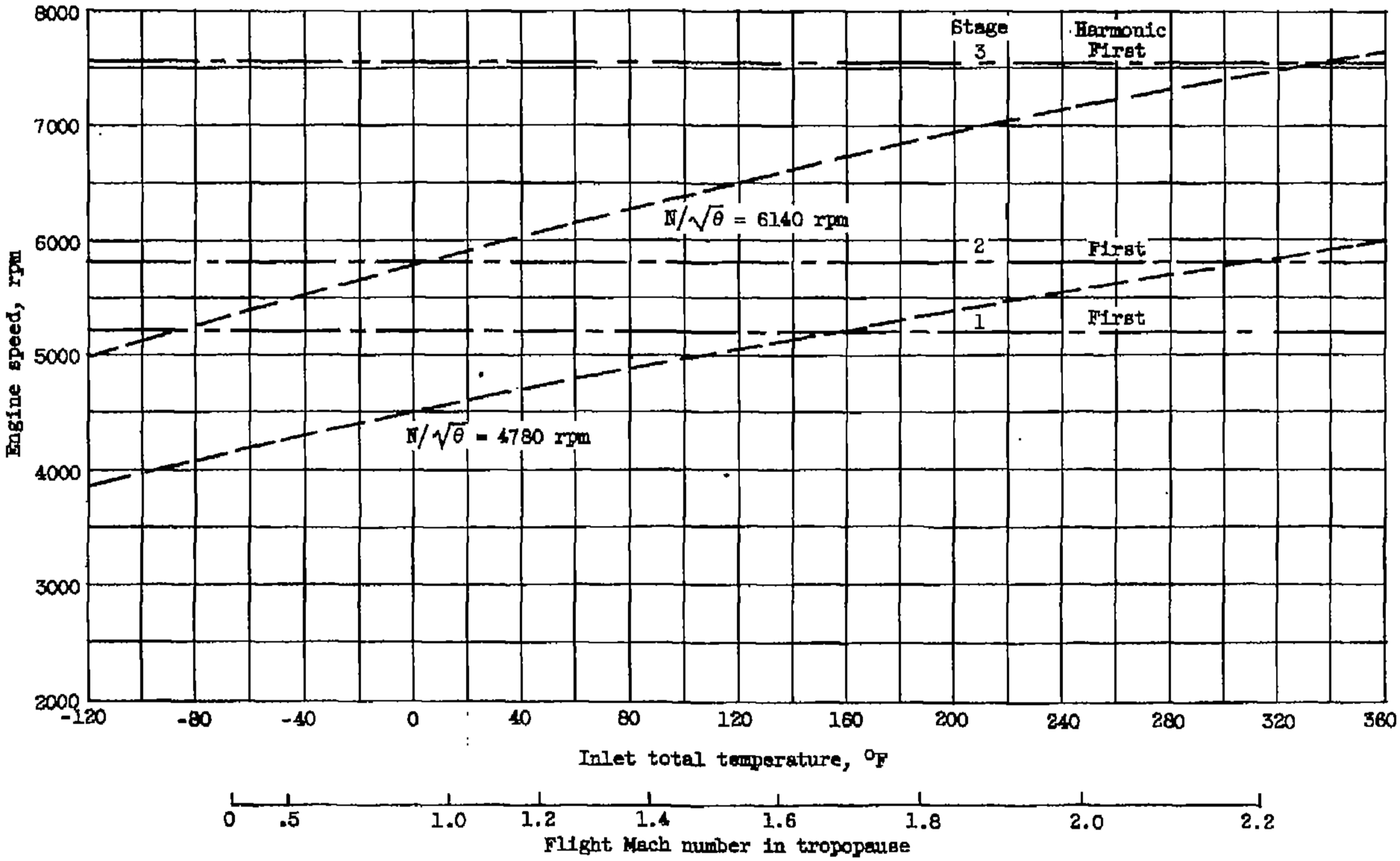

Figure 5. - Temperature range over which resonant vibrations due to three-zone stall pattern may be encountered.

3605

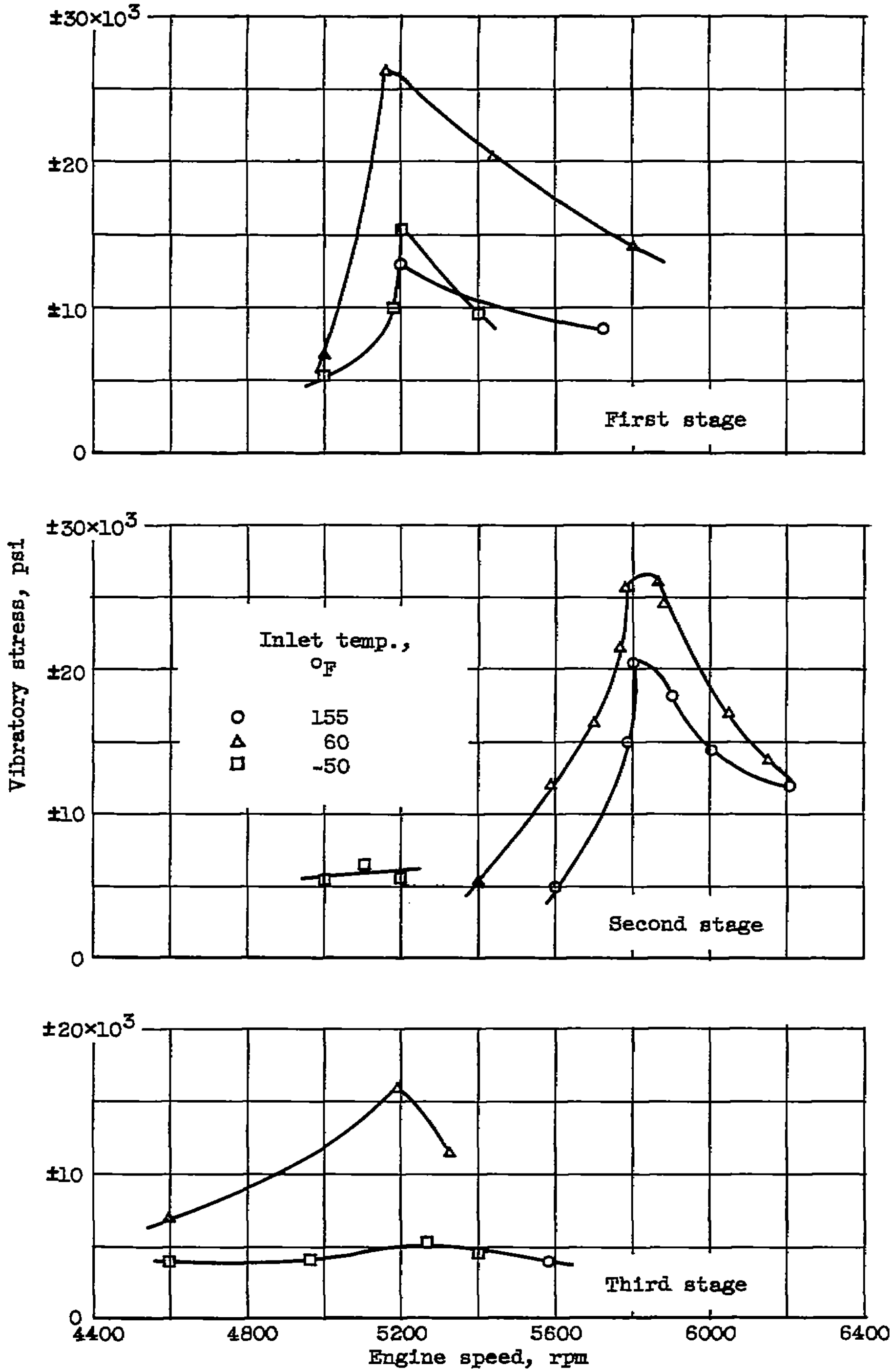

Figure 6. Vibratory stress in first three rotor blade rows as function of engine speed.

NACA - Langley Field, Va.